

**Gram-Scale Production of Fe Single Atom Catalyst and Mass Transfer
Enhancement in PEMFC**

Weikang Zhu^{1,2,}, Yuankai Shao^{1,2}, Bingjie Zhou^{1,2}, Shuoyao Yin^{1,2}, Anqi Dong^{1,2}, Yatao
Liu^{1,2}, Xi Liu^{1,2}, Zhenguo Li^{1,2,*}*

¹ National Engineering Laboratory for Mobile Source Emission Control Technology,
China Automotive Technology & Research Center Co., Ltd, Tianjin 300300, China

² Low-carbon Environmental Protection Department, CATARC Automobile Inspection
Center (Tianjin) Co., Ltd, Tianjin, 300300, China

*E-mail: lizhenguo@catarc.ac.cn (Z. Li); zhuweikang@catara.ac.cn (W. Zhu)

Synthesis of carbon support

The carbon support was synthesized according to our previous research with some modifications. Typically, 1.94 g (10 mM) anhydrous zinc acetate ($\text{Zn}(\text{OAc})_2$) was ultrasonically dispersed in 100 mL ultrapure water for 5 min. Another 100 mL ultrapure water containing 6.16 g (75 mM) 2-methylimidazole was also added into the above solution following by continuously stirring at room temperature for 4 h to obtain ZIF-8 precursor. After washing and drying, the white power was grinded with KCl (ZIF:KCl=1:5, weight) and transferred into tubular furnace. Then, the mixture was pyrolyzed at 800 °C for 2 h. After acid washing and drying, the black carbon support can be obtained for following Fe single atom active site loading.

Synthesis of Fe single atom catalyst

100 mg carbon support was separated in 50 mL ultrapure water. After adding 100 μL Fe-aqueous solution containing 10.56 mg (0.038 mM) ferrous sulfate heptahydrate ($\text{FeSO}_4 \cdot 7\text{H}_2\text{O}$) and 20.54 mg (0.114 mM) 1,10-phenanthroline, the mixture was ultrasonic treatment for 10 min and stirring for another 10 h. After separation and drying, the black power was annealing at specific temperature for 1 h to obtained the final Fe-based catalysts. The annealing temperature was sat at 800, 850, 900, 950 and 1000 °C, denoted as Fe/MNC-800, Fe/MNC-850, Fe/MNC-900, Fe/MNC-950 and Fe/MNC-1000, respectively.

Characterization

Scanning electron microscope (SEM) images were obtained on an Apreo S (Thermo Fisher Scientific, America) at an acceleration voltage of 2 kV, 100 pA. Transmission electron microscope (TEM) images were obtained on JEM-F200 FE-TEM (JEOL, Japan) instrument, and the relative amount as well as distribution of different elements were obtained by an energy dispersive X-ray detector attached to TEM. X-ray diffraction (XRD) patterns of supports and catalysts were obtained on a diffractometer (Bruker D8-Focus, Germany) using the $\text{Cu K}\alpha$ radiation ($k = 0.15418$). X-ray photoelectron spectra (XPS) patterns were recorded using an X-ray Photoelectron

Spectrometer (Thermo ESCALAB 250XI, USA) with an aluminum (mono) K α source (1486.6 eV). N₂ adsorption–desorption isotherms of different samples were measured by ASAP 2460 (Micromeritics, America). The specific surface area and pore size distribution were calculated based on the Brunauer–Emmett–Teller (BET) method and the nonlocal density functional theory (NLDFT) method. Contact angle was observed by SDC-350 contact angle meter (SINDIN Group, China). The pore size distribution and calculated porosity were obtained by a AutoPore V 9620 (Micromeritics, America).

XAS analysis

Data reduction, data analysis, and EXAFS fitting were performed and analyzed with the Athena and Artemis programs of the Demeter data analysis packages (*Journal of Synchrotron Radiation*, 2005, 12, 537–541) that utilizes the FEFF6 program (*Phys. Rev. B*, 1995, 52 (4), 2995–3009) to fit the EXAFS data. The energy calibration of the sample was conducted through standard Fe foil, which as a reference was simultaneously measured. A linear function was subtracted from the pre-edge region, then the edge jump was normalized using Athena software. The $\chi(k)$ data were isolated by subtracting a smooth, third-order polynomial approximating the absorption background of an isolated atom. The k^2 -weighted $\chi(k)$ data were Fourier transformed after applying a HanFeng window function ($\Delta k = 1.0$). For EXAFS modeling, the global amplitude EXAFS (CN, R, σ^2 and ΔE_0) were obtained by nonlinear fitting, with least-squares refinement, of the EXAFS equation to the Fourier-transformed data in R-space, using Artemis software, EXAFS of the Fe foil was fitted and the obtained amplitude reduction factor S_0^2 value (0.713) was set in the EXAFS analysis to determine the coordination numbers (CNs) in sample.

Electrochemical test

All the electrochemical data was obtained at 25 °C using a CHI 660E electrochemical workstation with a standard three-electrode system. The electrodes were a graphite rod,

a saturated calomel electrode (in saturated KCl solution, SCE), and a glassy carbon rotating disk electrode (RDE) coated with thin catalyst film, which served as the counter, reference, and working electrodes, respectively. To prepare catalyst-ionomer ink, 5 mg Fe single atom catalyst was dispersed in 1 mL mixed dispersant (40 μL 5 wt.% Nafion, 730 μL isopropanol and 230 μL ultrapure water). After 1 h ultrasonically treatment, 25 μL homogeneous ink was dropped on glassy carbon surface of RDE and dried naturally. Linear sweep voltammetry (LSV) was carried out in oxygen and nitrogen-saturated 0.1 M HClO_4 solution at 1600 rpm, 10 mV s^{-1} from 1.1 to 0.2 V versus reversible hydrogen electrode (RHE), and the effect of double layer capacitance was deducted. The accelerated degradation test (ADT) was conducted under O_2 -free 0.1 M HClO_4 solution with cyclic voltammetry (CV) method from 0.3 V to 1.1 V versus RHE. The LSV curves were recorded before and after ADT to evaluate the stability of Fe-based catalysts.

Fuel cell test

For the PEMFC tests, 48 mg Fe single atom catalyst was ultrasonically dispersed in a mixture of Nafion ionomer (5 wt.%, 411.4 mg), 9 mL isopropanol and 0.9 mL water to obtain the cathode ink. To reduce the contact resistance between the catalyst layer and membrane, the specific amount ink was sprayed onto one side of a clean Gore proton exchange membrane (12 μm) with an active area of 4 cm^2 at 80 $^\circ\text{C}$. A piece (2 \times 2 cm^2) of laboratory-made gas diffusion electrode (Johnson Matthey 40 wt.% Pt/C, 0.10 $\text{mg}_{\text{Pt}} \text{cm}^{-2}$) was employed as the anode electrode. After that, the membrane and gas diffusion layers were assembled and evaluated by a fuel cell test station. A constant gas flow of H_2 (300 sccm) – O_2 (500 sccm) or H_2 (300 sccm) – air (1500 sccm) was applied to the anode and cathode, respectively, with 100% relative humidity and 100 kPa backpressure at 80 $^\circ\text{C}$. The galvanostatic tests were carried out under 500 mA cm^{-2} to evaluate the stability of Fe-based PEMFC with different GDLs.

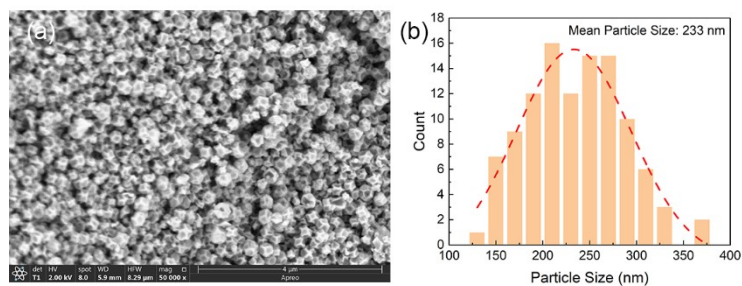


Figure S1. (a) SEM morphology and (b) statistics histogram of MNC which was pyrolyzed at 800 °C for 2 h.

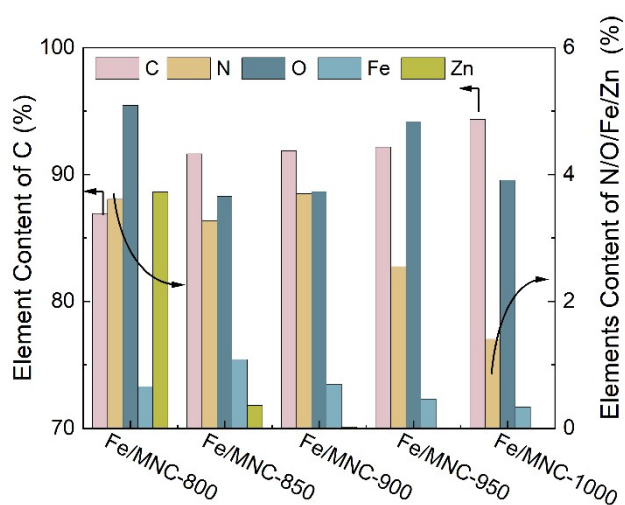


Figure S2. The elements contents of C, N, O, Fe and Zn via TEM-EDS test.

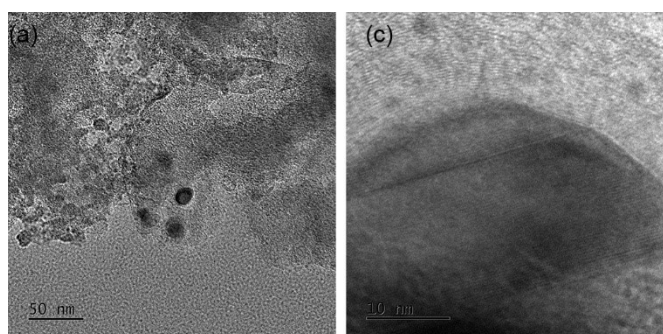


Figure S3. The TEM images of Fe/MNC-1000 catalyst.

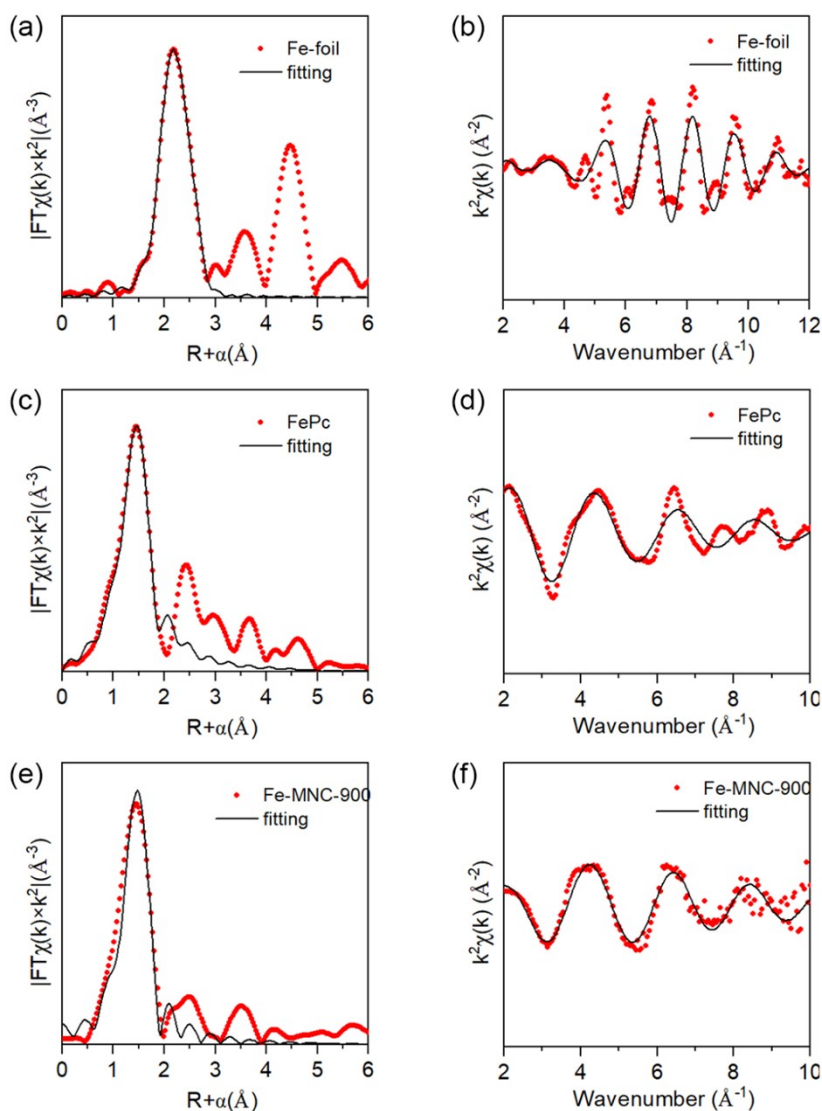


Figure S4. The Fe K-edge EXAFS (red) and fitting (black) of (a, b) Fe-foil (c, d) FePc and (e, f) Fe/MNC-900 shown in k^2 weighted (left) k -space and (right) R -space.

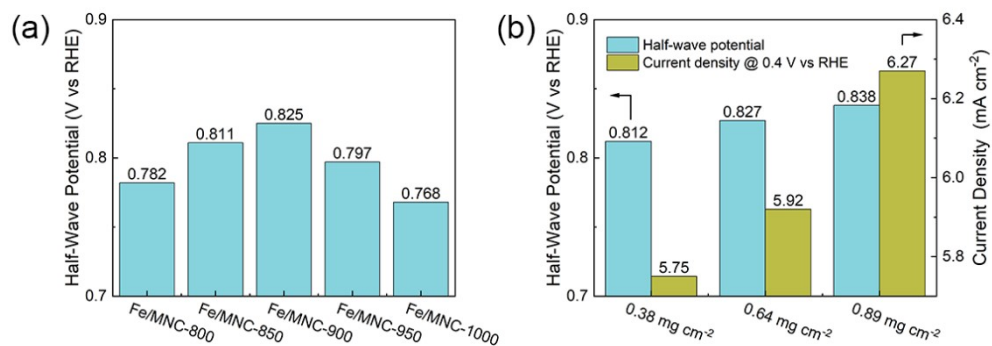


Figure S5. ORR performance of (a) different catalyst and (b) g-level Fe/MNC-900 with different catalyst loading via RDE LSV test.

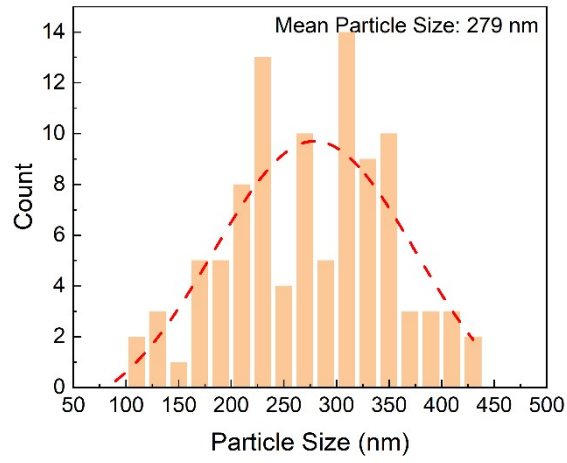


Figure S6. Statistics histogram of g-level ZIF precursor production.

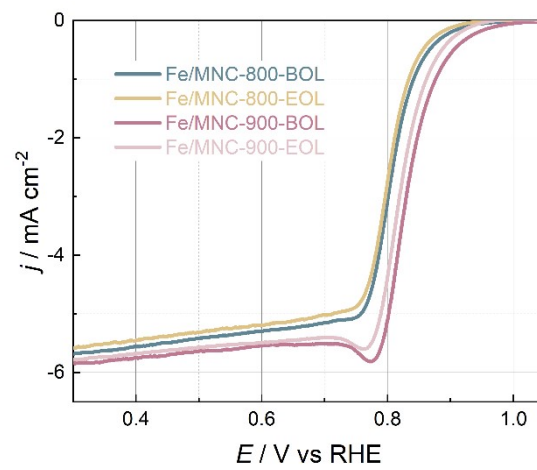


Figure S7. The LSV curves of Fe/MNC-800 and Fe/MNC-900 catalysts before and after 5000 cycles CV scanning from 0.3 V to 1.1 V vs RHE.

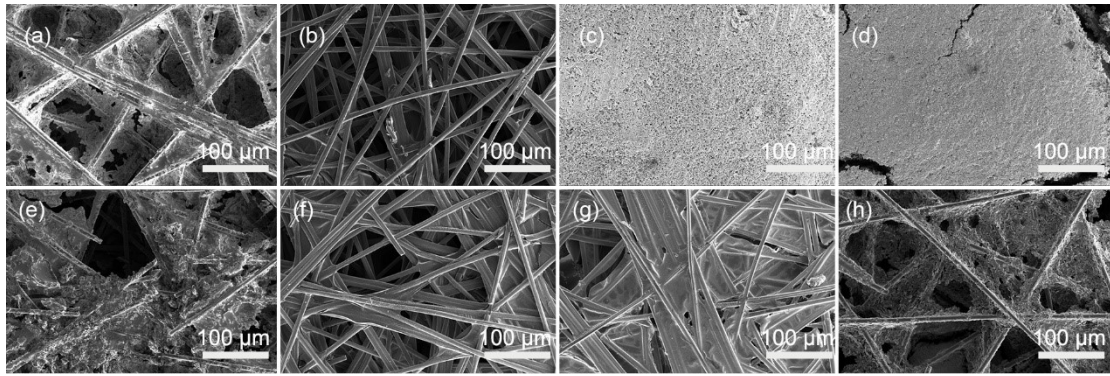


Figure S8. SEM images of (a, e) AvCarb P40T, (b, f) Toray 060, (c, g) TF120 and (d, h) SGL 22BB. (a to d) are the surface morphology of MEA side and (e to h) are the follow channel side.

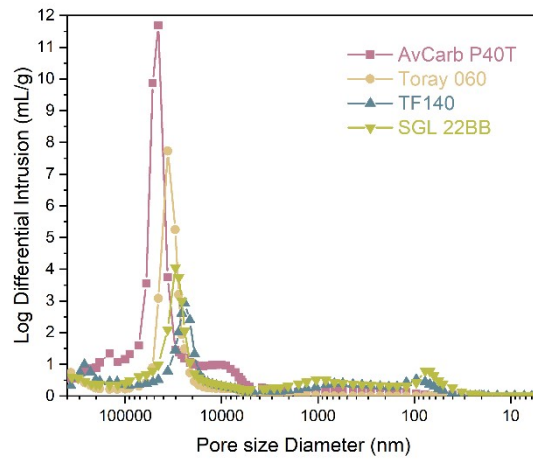


Figure S9. Pore size distribution of different GDLs via mercury injection test.

Table S1. The percentage of N-based species in different catalysts via XPS test.

	pyri-N (N-1)	M-N (N-2)	pyrr-N (N-2)	grap-N (N-3)	oxy-N (N-4)
MNC	36.47	17.87	23.05	13.34	9.27
Fe/MNC-800	33.48	21.75	14.06	13.58	17.13
Fe/MNC-850	34.67	20.37	16.05	16.05	12.87
Fe/MNC-900	33.04	19.59	12.48	16.43	18.46
Fe/MNC-950	26.70	16.29	15.40	24.62	17.00
Fe/MNC-1000	16.71	11.62	15.03	27.08	29.56

Table S2. The percentage of Fe²⁺ and Fe³⁺ in different catalysts via XPS test.

	Fe ²⁺	Fe ³⁺	Fe ³⁺ /Fe ²⁺
MNC	/	/	/
Fe/MNC-800	35.63	64.37	1.81
Fe/MNC-850	33.47	66.53	1.99
Fe/MNC-900	23.43	76.57	3.27
Fe/MNC-950	24.64	75.36	3.06
Fe/MNC-1000	49.50	50.50	1.02

Table S3. EXAFS fitting parameters at the Fe K-edge for various samples.

Sample	Shell	CN ^a	R(Å) ^b	$\sigma^2(\text{Å}^2)$ ^c	$\Delta E_0(\text{eV})$ ^d	K-range/Å ⁻¹	R-range/Å	R factor
Fe-foil	Fe-Fe	8*	2.45±0.01	0.0054±0.0012	3.7±0.7	2.3-12.0	1.3-3.0	0.0082
	Fe-Fe	6*	2.82±0.01	0.0045±0.0012	3.3±0.9			
FePc	Fe-N	4*	1.97±0.01	0.0059±0.0018	0.7±0.5	2.0-10.0	1.0-2.0	0.0074
Fe/MNC-900	Fe-N	4.2±0.7	1.99±0.01	0.0082±0.0032	-2.6±0.7	2.0-10.0	1.0-2.0	0.0154

^aCN, coordination number;

^bR, the distance between absorber and backscatter atoms;

^c σ^2 , Debye-Waller factor, Debye-Waller factor to account for both thermal and structural disorders;

^d ΔE_0 , inner potential correction; R factor indicates the goodness of the fit. S_0^2 was fixed to 0.713, according to the experimental EXAFS fit of Fe foil by fixing CN as the known crystallographic value. Error bounds that characterize the structural parameters obtained by EXAFS spectroscopy were estimated as CN±20%; R±1%; σ^2 ±20%; ΔE_0 ±20%. A reasonable range of EXAFS fitting parameters: $0.700 < S_0^2 < 1.000$; $CN > 0$; $\sigma^2 > 0 \text{ Å}^2$; $|\Delta E_0| < 15 \text{ eV}$; R factor < 0.02.

Table S4. The comparison of ORR key parameters with previous research.

Catalyst	BET specific surface area (m ² g ⁻¹)	RDE test		PEMFC test			Ref.
		Catalyst loading in RDE (mg cm ⁻²)	Half-wave potential (V vs RHE)	Catalyst in Anode (mg cm ⁻²)	Catalyst loading in cathode (mg cm ⁻²)	Maximum power density (W cm ⁻²)	
Fe/N-PCNs	864	0.51	0.79 , 0.1 M HClO ₄	/	/	/	[1]
Mn-N-C-HCl-800/1100	1511	0.8	0.815 , 0.5 M H ₂ SO ₄	0.3 mg _{Pt} cm ⁻² Pt/C electrode	4.0	0.6 , H ₂ -O ₂ , 150 kPa _{abs}	[2]
M/FeCo-Sas-N-C	1003.7	0.6	0.851 , 0.1 M HClO ₄	/	/	/	[3]
Zn/CoN-C	1343	0.255	0.796 , 0.1 M HClO ₄	/	/	0.705 , H ₂ -O ₂	[4]
Fe _{SA} -N-C	1615	~0.28	0.80 , 0.1 M HClO ₄	0.2 mg _{Pt} cm ⁻² Pt/C electrode	3.0	0.68 , H ₂ -O ₂ , 150 kPa (backpressure)	[5]
Fe SAC-MOF-5	2751	0.8	0.83 , 0.5 M H ₂ SO ₄	0.1 mg _{Pt} cm ⁻² (JM 20% PtRu/C)	4.0	0.84 , H ₂ -O ₂ , 200 kPa _{abs}	[6]
FeN ₄ -HS	370.2	0.1	0.78 , 0.1 M HClO ₄	0.2 mg _{Pt} cm ⁻² 40% Pt/C electrode	4.0	0.500 , H ₂ -O ₂ , 200 kPa _{abs}	[7]
Co-N/C-1/4.4	695.7	0.8	0.781 , 0.1 M HClO ₄	0.4 mg _{Pt} cm ⁻² 40% Pt/C electrode	3.5	1.12 , H ₂ -O ₂ , 200 kPa _{abs}	[8]
Fe/MNC-900	1450.7	0.64	0.825 , 0.1 M HClO ₄	0.1 mg _{Pt} cm ⁻² (JM 40% Pt/C)	1.2	0.803 , H ₂ -O ₂ , 150 kPa _{abs}	This work

Reference

1. Zheng, L.; Yu, S.; Lu, X.; Fan, W.; Chi, B.; Ye, Y.; Shi, X.; Zeng, J.; Li, X.; Liao, S., *ACS Appl. Mater. Interfaces* **2020**, *12* (12), 13878-13887.
2. Chen, M.; Li, X.; Yang, F.; Li, B.; Stracensky, T.; Karakalos, S.; Mukerjee, S.; Jia, Q.; Su, D.; Wang, G.; Wu, G.; Xu, H., *ACS Catal.* **2020**, *10* (18), 10523-10534.
3. Yin, S.-H.; Yang, J.; Han, Y.; Li, G.; Wan, L.-Y.; Chen, Y.-H.; Chen, C.; Qu, X.-M.; Jiang, Y.-X.; Sun, S.-G., *Angew. Chem. Inter. Ed.* **2020**, *59* (49), 21976-21979.
4. Lu, Z.; Wang, B.; Hu, Y.; Liu, W.; Zhao, Y.; Yang, R.; Li, Z.; Luo, J.; Chi, B.; Jiang, Z.; Li, M.; Mu, S.; Liao, S.; Zhang, J.; Sun, X., *Angew. Chem. Inter. Ed.* **2019**, *58* (9), 2622-2626.
5. Jiao, L.; Zhang, R.; Wan, G.; Yang, W.; Wan, X.; Zhou, H.; Shui, J.; Yu, S. H.; Jiang, H. L., *Nat. Commun.* **2020**, *11* (1), 2831.
6. Xie, X.; Shang, L.; Xiong, X.; Shi, R.; Zhang, T., *Adv. Energy Mater.* **2022**, *12* (3), 2102688.
7. Xue, D.; Yuan, P.; Jiang, S.; Wei, Y.; Zhou, Y.; Dong, C.-L.; Yan, W.; Mu, S.; Zhang, J.-N., *Nano Energy* **2023**, *105*.
8. Qu, X.-M.; Yin, S.-H.; Yan, Y.-N.; Yang, J.; Li, Y.-R.; Cheng, X.-Y.; Lu, F.; Wang, C.-T.; Jiang, Y.-X.; Sun, S.-G., *Chem. Eng. J.* **2023**, *461*.